Vol. 20, e200035 (2023)
doi: 10.2142/biophysico.bppb-v20.0035

Biophysics and Physicobiology
https://www.jstage.jst.go.jp/browse/biophysico/

Review Article (Invited)

Description of peptide bond planarity from high-resolution neutron crystallography

Yuya Hanazono[1], Yu Hirano[2,3], Taro Tamada[2,3], Kunio Miki[4]

[1] *Medical Research Institute, Tokyo Medical and Dental University, Bunkyo-ku, Tokyo 113-8510, Japan*
[2] *Institute for Quantum Life Science, National Institutes for Quantum Science and Technology, Inage-ku, Chiba 263-8555, Japan*
[3] *Department of Quantum Life Science, Graduate School of Science, Chiba University, Inage-ku, Chiba 263-8522, Japan*
[4] *Department of Chemistry, Graduate School of Science, Kyoto University, Sakyo-ku, Kyoto 606-8502, Japan*

Received May 31, 2023; Accepted September 4, 2023;
Released online in J-STAGE as advance publication September 6, 2023
Edited by Takeshi Murata

Neutron crystallography is a highly effective method for visualizing hydrogen atoms in proteins. In our recent study, we successfully determined the high-resolution (1.2 Å) neutron structure of high-potential iron-sulfur protein, refining the coordinates of some amide protons without any geometric restraints. Interestingly, we observed that amide protons are deviated from the peptide plane due to electrostatic interactions. Moreover, the difference in the position of the amide proton of Cys75 between reduced and oxidized states is possibly attributed to the electron storage capacity of the iron-sulfur cluster. Additionally, we have discussed about the rigidity of the iron-sulfur cluster based on the results of the hydrogen-deuterium exchange. Our research underscores the significance of neutron crystallography in protein structure elucidation, enriching our understanding of protein functions at an atomic resolution.

Key words: high-resolution crystallography, iron-sulfur cluster, H/D exchange

Significance

The planarity of peptide bonds including hydrogen atoms is not fully understood. From the high-resolution neutron structure of high-potential iron-sulfur protein, we have determined the coordinates of hydrogen atoms without any geometric restraints and observed the deviation of amide protons from the peptide plane. Additionally, we discuss the rigidity around the iron-sulfur cluster from the result of the hydrogen-deuterium exchange ratio. The high rigidity around iron-sulfur cluster is important for the high redox potential.

Introduction

Hydrogen atoms, constituting nearly half of all the atoms in proteins, play a pivotal role in substrate recognition and catalytic reaction. However, due to their possession of only one electron, the determination of the coordinates using X-ray crystallography is difficult. Neutron crystallography leverages the interactions between neutron beams and atomic nuclei to determine the coordinates of hydrogen atoms with almost the same precision as those of other atoms such as

Corresponding author: Yuya Hanazono, Medical Research Institute, Tokyo Medical and Dental University, Bunkyo-ku, Tokyo 113-8510, Japan. ORCID iD: https://orcid.org/0000-0002-3102-2945

carbon, nitrogen, and oxygen [1,2]. Moreover, in neutron crystallography, the hydrogen (protium)-deuterium (H/D) exchange ratio can provide valuable information for understanding the conformational dynamics and exposure to water [3–6]. In neutron data collection, the H/D exchange procedure with D_2O solution is important to minimize background noise caused by the incoherent scattering of protium. This necessitates the replacement of protium with deuterium, given its significantly lower incoherent scattering properties. The exchange ratio can be determined by structure refinement because protium has a negative neutron scattering length while deuterium has a positive scattering length.

High-potential iron-sulfur protein (HiPIP) functions as an electron carrier within bacterial photosynthesis. It acquires an electron from the cytochrome bc_1 complex and transports it to light-harvesting antenna 1-reaction center complex (LH1-RC). At the center of HiPIP is a Fe_4S_4 cluster, which transitions between two different states: $[Fe_4S_4]^{3+}$ in its oxidized state, and $[Fe_4S_4]^{2+}$ when reduced. The redox potential of HiPIP exceeds +300 mV, a high value attributable to the hydrogen bonding and hydrophobic environment surrounding the iron-sulfur cluster. We have previously published our works on the X-ray crystal structures of both the reduced (~0.48 Å resolution) and oxidized (~0.80 Å resolution) states of HiPIP derived from a thermophilic purple bacterium, *Thermochromatium tepidum* [7–12]. Recently, we have collected neutron diffraction data at 1.2 Å resolution and X-ray diffraction data at 0.66 Å resolution for the oxidized state of HiPIP from *T. tepidum*, substantially high resolutions for protein structural research [13–15]. Generally, the coordinates of hydrogen atoms are constrained to ensure that the bond distances and angles with the atoms to which they are bonded maintain ideal geometries. This is known as the "riding model" [16,17]. Thanks to the high-resolution neutron diffraction data, we determined the coordinates of the amide protons for the first time without any geometric restraints in protein structure determination. As a result, we have experimentally demonstrated that peptide bonds, traditionally believed to have a planar structure, are influenced by the electronic interaction, and the amide protons are deviated from the peptide plane. In addition, the deviation of amide proton is correlated with the redox states of the iron-sulfur cluster. Furthermore, we discuss the structural rigidity around the iron-sulfur cluster of HiPIP as an outcome of H/D exchange.

The Deviation of Amide Proton from Peptide Plane

HiPIP was crystallized in a solution prepared with deuterated reagents and heavy water, yielding deuterium-substituted crystals. Neutron diffraction data were collected using the IBARAKI biological crystal diffractometer (iBIX) at BL03 of the Materials and Life Science Experimental Facility (MLF) at Japan Proton Accelerator Research Complex (J-PARC). X-ray diffraction data were also collected from the same crystal using an ADSC Q315r detector on BL5A at Photon Factory (PF). For structure refinement, we combined the neutron data (1.2 Å) and the X-ray data (0.66 Å). Initially, we performed the structure refinement without hydrogen atoms using only X-ray data. Subsequently, we determined the coordinates of hydrogen atoms using neutron data. Because the data-to-parameter ratio of the neutron data is enough to refine the crystallographic parameters of amide protons, we refined the coordinates of amide protons without geometric constraints for deuterium atoms with clear neutron scattering length density (nuclear density) and occupancy greater than 0.60, and protium atoms with occupancy greater than 0.75. The final R_{work} and R_{free} are 7.41% and 8.15% for the X-ray data and 15.4% and 16.8% for the neutron data, respectively. Each atom position was resolved in the electron and nuclear densities, and even the polarization of hydrogen atoms can be seen from the difference in the center of hydrogen atoms in neutron and X-ray data (Figure 1).

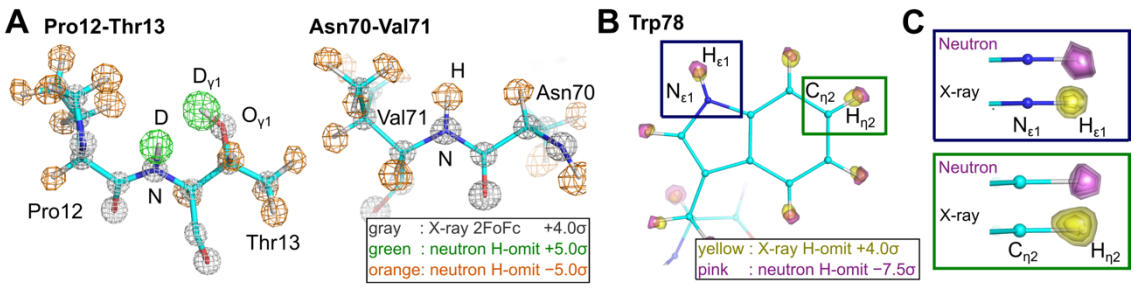

Figure 1 Electron and nuclear density of HiPIP [13]. (A) Electron and nuclear density maps around the peptide bond between Pro12 and Thr13, and between Asn70 and Val71. (B) Difference between the center of electron density and nuclear density of the indole ring of Trp78. (C) Close-up view of $N_{\varepsilon1}$—$H_{\varepsilon1}$ and $C_{\eta2}$—$H_{\eta2}$ of Trp78.

A typical hydrogen bond comprises a single acceptor-donor pair. However, there are instances where a hydrogen-bond pattern may include more than one donor or acceptor, forming what is known as a bifurcated hydrogen bond. In single-acceptor hydrogen bonds, the refined angles between donor, hydrogen, and acceptor (∠DH…A) typically exceed those

found in the riding model, with the nuclei of the amide protons generally exhibiting a shift towards the acceptor atoms (Figure 2). Conversely, in bifurcated hydrogen bonds, certain amide protons are displaced from the nearest acceptor atoms, indicating that these hydrogen atoms subject to the pull of electrostatic forces from two directions (Figure 2A). The planarity of the peptide bond has conventionally been evaluated using non-hydrogen atoms because little structural information is available for the amide proton. However, with the experimental determination of the position of the amide proton, we focused on the planar structure including the amide proton and defined the dihedral angle in the H_i─N_i─C_{i-1}═O_{i-1} plane, where i is the residue number, as ω′. The planarity of a double bond, reflecting the ratio of sp^2 hybrid orbitals, can be evaluated using the pyramidalization angle, θ [18]. The pyramidalization angle for carbon (θ_C) ranges from approximately -5° to 5°, suggesting near-planar conformation (Figure 3A). In addition, it exhibits no correlation with ω′. This stems from the robust maintenance of the sp^2 orbital of the carbon atoms by the C═O double bond. On the other hand, the pyramidalization angle for the amide nitrogen (θ_N) displays a broad range from -25° to 20° (Figure 3B) with θ_N exhibiting a strong correlation with ω′. This indicates that the pyramidalization of amide nitrogens occurs when amide protons are attracted to acceptors by electrostatic interactions, disrupting the planarity of H_i─N_i─C_{i-1}═O_{i-1} comprising the ω′ angle (Figure 3C).

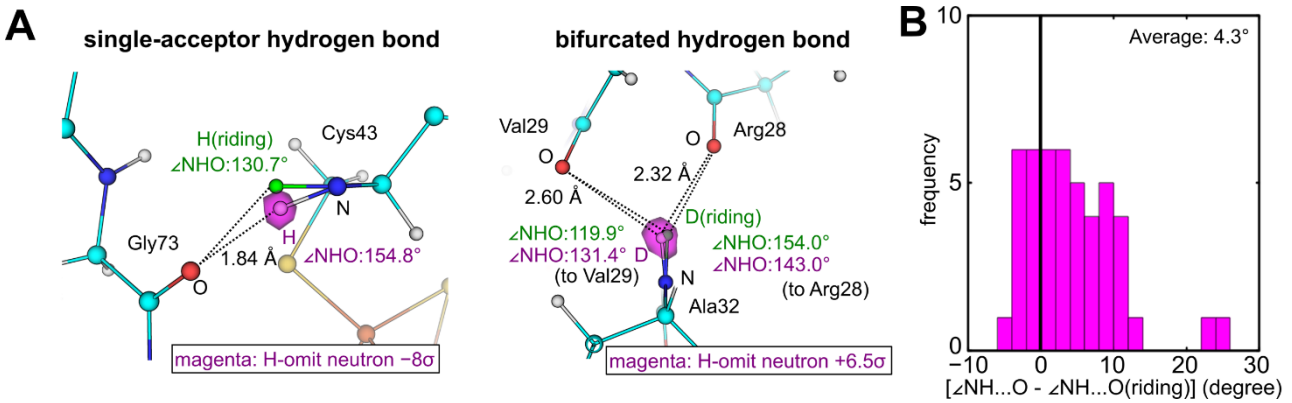

Figure 2 Difference between the refined model and riding model of amide protons. (A) Deviations of hydrogen atoms from the peptide plane in single-acceptor hydrogen bond (left) and bifurcated hydrogen bond (right). The hydrogen omit nuclear density map is shown in magenta. The amide hydrogen atoms of riding models are shown in green. The distance between amide proton and oxygen atoms are shown in black. The angles of NH…O for experimentally determined models and riding models are shown in magenta and green, respectively. (B) Histogram of the frequency of differences in donor-hydrogen acceptor angles in single-acceptor hydrogen bonds between the experimentally refined model and the riding model. (This figure is modified from ref. [13].)

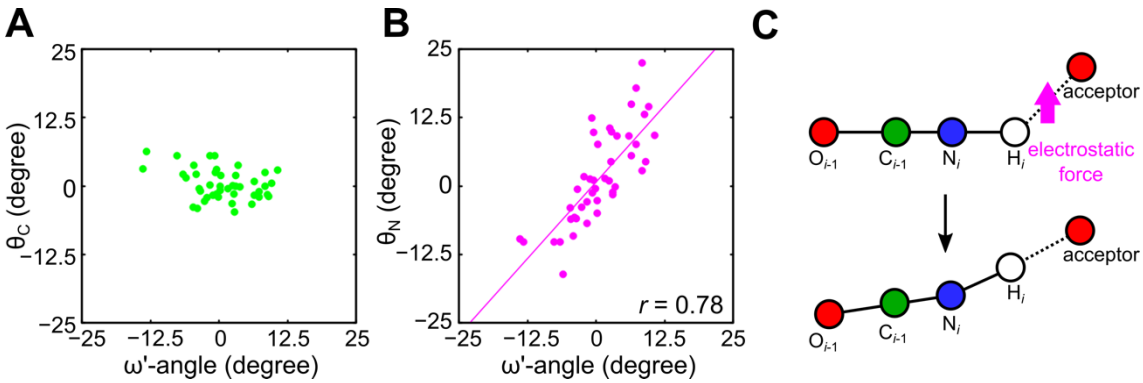

Figure 3 Deviation of amide protons [13]. (A) Scatter plot of θ_C against ω′-angle. (B) Scatter plot of θ_N against ω′-angle. Linear regression is shown as a solid line. (C) Side-view schematic of the peptide bond. The attraction of the amide proton by the acceptor atom shifts the H_i─N_i─C_{i-1}═O_{i-1} plane.

Relationship between the Non-planarity of Peptide Bonds and Protein Function

The deviation of amide protons from the peptide plane has a strong correlation with the redox state of HiPIP. The Fe_4S_4 cluster can be divided into two subclusters based on the form of spin coupling between iron atoms. Subcluster 1, formed by Fe1-S4-Fe2-S3, plays a pivotal role in electron storage [10]. In the oxidized state of HiPIP, the amide protons of Cys75 are not oriented toward the S3 atom due to the distortion of the peptide bond near the Fe_4S_4 cluster, instead forming NH-π interactions with the indole ring of Trp74 (Figure 4). In contrast, in the reduced form (X-ray structure at 0.48 Å resolution [10]), the orientation of the N─H bond is nearly aligned with the peptide plane and interacts with the S3 atom. Since the reduced form carries an extra electron compared to the oxidized form, the amide proton of Cys75 is attracted to the S3 atom in subcluster 1, stabilizing the $[Fe_4S_4]^{2+}$ state. This implies that the orientation of a single amide proton interacting with the Fe_4S_4 cluster may regulate electron transfer in HiPIP.

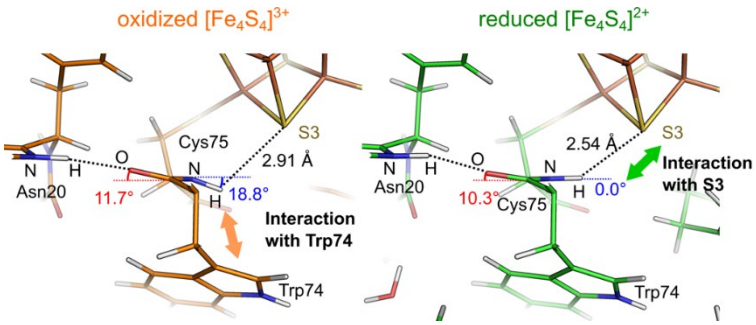

Figure 4 Difference of the amide proton of Cys75. (left) Position of the amide proton of Cys75 in the oxidized state. (right) Positions of the amide proton of Cys75 in the reduced state (PDB ID: 5D8V). (This figure is modified from ref. [13].)

Structural Rigidity around Iron-Sulfur Cluster of HiPIP

In this study, we collected neutron diffraction data from the crystal prepared with deuterated reagents and heavy water, which provided information about the H/D exchange ratio of each exchangeable hydrogen atom. Most protium atoms of surface residues were exchanged with deuterium atoms, while protium atoms around the iron-sulfur cluster did not undergo H/D exchange (Figure 5A, B). Notably, the amide protons in the contiguous region around Cys61 and Cys75 remained their protium atoms. Moreover, the amide protons of residues 11–20, which interact with residues 72–76, were not exchanged with deuterium atoms, while those in regions of residues 27–32 (forming a helical structure) and 49–58 (forming a β-sheet-like conformation) exchanged. These observations suggest that the hydrophobic core is highly rigid and that solvent molecules cannot access the iron-sulfur cluster. The Fe_4S_4 cluster of HiPIP is entirely enclosed with hydrophobic residues (Figure 5C). In contrast, the Fe_4S_4 cluster of bacterial-type ferredoxins is exposed to the solvent and exhibits a substantially lower redox potential. The hydrophobicity of this region is strictly conserved among HiPIPs (Figure 5D), and these conserved regions showed a strong correlation with the H/D exchange ratio (Figure 5A). These findings suggest that the Fe_4S_4 cluster of HiPIP is firmly retained within a hydrophobic environment, and the high rigidity of the hydrophobic core surrounding the cluster plays a crucial role in maintaining its high redox potential in solution.

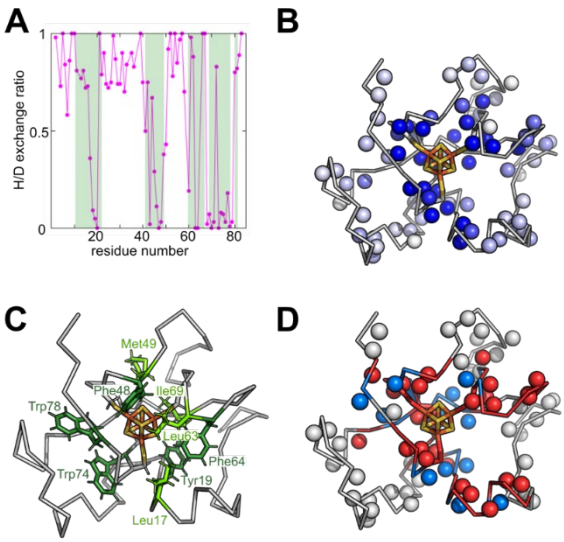

Figure 5 H/D exchange of HiPIP. (A) H/D exchange ratio of amide proton of oxidized HiPIP. The regions of sequence conserved residues are colored in green. (B) Mapping of the H/D exchange ratio on the structure. The gradations of color from white to blue correspond to the ratio of protium atom from 0 to 1. (C) Hydrophobic core around iron-sulfur cluster. The hydrophobic and aromatic residues are colored in light green and dark green, respectively. (D) Mapping of the sequence conservation. The highly conserved and moderately conserved residues are colored in red and blue, respectively.

Conflict of Interest

The authors declare that there are no conflicts of interest.

Author Contributions

Y.Hanazono wrote the initial manuscript and all authors revised and approved the manuscript.

Data Availability

The evidence data generated and/or analyzed during the current study are available from the corresponding author on reasonable request.

Acknowledgements

The content presented in this paper is based in part on collaborative research with Dr. Kazuki Takeda from Kyoto University and Dr. Katsuhiro Kusaka from Comprehensive Research Organization for Science and Society. Furthermore, we would like to thank Dr. Kazuo Kurihara from National Institutes for Quantum Science and Technology and the staff of J-PARC MLF and PF for their assistance with the diffraction experiments.

References

[1] Kono, F., Tamada, T. Neutron crystallography for the elucidation of enzyme catalysis. Curr. Opin. Struct. Biol. 71, 36–42 (2021). https://doi.org/10.1016/j.sbi.2021.05.007

[2] Kono, F., Kurihara, K., Tamada, T. Current status of neutron crystallography in structural biology. Biophys. Physicobiol. 19, e190009 (2022). https://doi.org/10.2142/biophysico.bppb-v19.0009

[3] Kossiakoff, A. A. Protein dynamics investigated by the neutron diffraction–hydrogen exchange technique. Nature 296, 713–721 (1982). https://doi.org/10.1038/296713a0

[4] Fukuda, Y., Hirano, Y., Kusaka, K., Inoue, T., Tamada, T. High-resolution neutron crystallography visualizes an OH-bound resting state of a copper-containing nitrite reductase. Proc. Natl. Acad. Sci. U.S.A. 117, 4071–4077 (2020). https://doi.org/10.1073/pnas.1918125117

[5] Wan, Q., Parks, J. M., Hanson, B. L., Fisher, S. Z., Ostermann, A., Schrader, T. E., et al. Direct determination of protonation states and visualization of hydrogen bonding in a glycoside hydrolase with neutron crystallography. Proc. Natl. Acad. Sci. U.S.A. 112, 12384–12389 (2015). https://doi.org/10.1073/pnas.1504986112

[6] Sukumar, N., Mathews, F. S., Langan, P., Davidson, V. L. A joint x-ray and neutron study on amicyanin reveals the role of protein dynamics in electron transfer. Proc. Natl. Acad. Sci. U.S.A. 107, 6817–6822 (2010). https://doi.org/10.1073/pnas.0912672107

[7] Nogi, T., Fathir, I., Kobayashi, M., Nozawa, T., Miki, K. Crystal structures of photosynthetic reaction center and high-potential iron-sulfur protein from *Thermochromatium tepidum*: thermostability and electron transfer. Proc. Natl. Acad. Sci. U.S.A. 97, 13561–13566 (2000). https://doi.org/10.1073/pnas.240224997

[8] Liu, L., Nogi, T., Kobayashi, M., Nozawa, T., Miki, K. Ultrahigh-resolution structure of high-potential iron-sulfur protein from *Thermochromatium tepidum*. Acta Crystallogr. D, Biol. Crystallogr. 58, 1085–1091 (2002). https://doi.org/10.1107/s0907444902006261

[9] Takeda, K., Kusumoto, K., Hirano, Y., Miki, K. Detailed assessment of X-ray induced structural perturbation in a crystalline state protein. J. Struct. Biol. 169, 135–144 (2010). https://doi.org/10.1016/j.jsb.2009.09.012

[10] Hirano, Y., Takeda, K., Miki, K. Charge-density analysis of an iron-sulfur protein at an ultra-high resolution of 0.48 Å. Nature 534, 281–284 (2016). https://doi.org/10.1038/nature18001

[11] Ohno, H., Takeda, K., Niwa, S., Tsujinaka, T., Hanazono, Y., Hirano, Y., et al. Crystallographic characterization of the high-potential iron-sulfur protein in the oxidized state at 0.8 Å resolution. PLoS One 12, e0178183 (2017). https://doi.org/10.1371/journal.pone.0178183

[12] Hanazono, Y., Takeda, K., Miki, K. Characterization of perdeuterated high-potential iron-sulfur protein with high-resolution X-ray crystallography. Proteins 88, 251–259 (2020). https://doi.org/10.1002/prot.25793

[13] Hanazono, Y., Hirano, Y., Takeda, K., Kusaka, K., Tamada, T., Miki, K. Revisiting the concept of peptide bond planarity in an iron-sulfur protein by neutron structure analysis. Sci. Adv. 8, eabn2276 (2022). https://doi.org/10.1126/sciadv.abn2276

[14] Hanazono, Y., Hirano, Y., Tamada, T., Miki, K. New description of the peptide bond in proteins revealed by high-resolution neutron crystallography. Nihon Kesshō Gakkaishi 64, 207–208 (2022).

https://doi.org/10.5940/jcrsj.64.207
[15] Hanazono, Y., Hirano, Y., Tamada, T., Miki, K. Revisiting the peptide bond planarity by high-resolution neutron crystallography. SEIBUTSU BUTSURI 63, 205–206 (2023). https://doi.org/10.2142/biophys.63.205
[16] Liebschner, D., Afonine, P. V, Urzhumtsev, A. G., Adams, P. D. Implementation of the riding hydrogen model in CCTBX to support the next generation of X-ray and neutron joint refinement in Phenix. Methods Enzymol. 634, 177–199 (2020). https://doi.org/10.1016/bs.mie.2020.01.007
[17] Sheldrick, G. M. Crystal structure refinement with *SHELXL*. Acta Crystallogr. C, Struct. Chem. 71, 3–8 (2015). https://doi.org/10.1107/S2053229614024218
[18] Ramachandran, G. N., Kolaskar, A. S. The non-planar peptide unit II. Comparison of theory with crystal structure data. Biochim. Biophys. Acta 303, 385–388 (1973). https://doi.org/10.1016/0005-2795(73)90374-7